https://doi.org/10.5194/egusphere-2026-1718
Preprint. Discussion started: 24 April 2026

Impact of light, turbulent mixing, and nutrients on phytoplankton photoinhibition in the euphotic zone from the subtropical to subpolar North Atlantic

Jørgen Bendtsen[1,2], Line D. Jessen[3], Niels Daugbjerg[4], Katherine Richardson[3]

[1]Globe Institute, Section for Geobiology, University of Copenhagen, Øster Voldgade 5-7, DK-1350 Copenhagen K, Denmark
[2]ClimateLab, Symbion Science Park, Fruebjergvej 3, DK-2100 Copenhagen Ø, Denmark
[3]Globe Institute, Section for Biodiversity, University of Copenhagen, Universitetsparken 15, DK-2100 Copenhagen Ø, Denmark
[4]Department of Biology, University of Copenhagen, Universitetsparken 4, DK-2100 Copenhagen Ø, Denmark

Correspondence to: Jørgen Bendsten (jb@climatelab.dk)

Abstract.

Photoinhibition, a condition caused when high photon fluxes lead to the rate of electron transport from light receptors in photosystem II exceeding a cell's photochemical capacity, causes damage to the photosynthetic apparatus and reduces photosynthesis. The balance between damage and repair processes in cells determines the degree of photoinhibition (PI). PI is here shown to be ubiquitous in natural phytoplankton communities in the North Atlantic. PI effects were determined as the difference between the maximum photosynthetic quantum yield (F_v/F_m) recorded at the time of sampling and following a 4 h low-light incubation. Samples from the euphotic zone in the North Sea showed significant daily variation of PI extending to depths of 20 m. Principal component analysis identified a strong correlation between PI and light availability, whereas nutrient distributions and other environmental variables were less influential on PI. Furthermore, an almost immediate response of PI to changes in light intensity was demonstrated. A light-dependent linear regression model of PI for the northern North Sea explained a significant increase in PI ($R^2 = 0.4$) with intensity of insolation. PI in samples from the euphotic zone in the subpolar Irminger Sea and the subtropical Sargasso Sea also showed significantly elevated PI at higher light levels. Our results show that PI in natural phytoplankton communities is closely related to, and occurs almost immediately, in response to changes in insolation. The sensitivity of phytoplankton communities' photo-chemical capacity to insolation changes may help to explain the wide variation in photosynthetic parameters reported in nature and should be taken into account when estimating ocean primary production.

1 Introduction

Chlorophyll molecules in photosystem II (PS II) in all photosynthesizing cells absorb light and induce an electron transport that is directed towards growth and metabolic consumption, fluorescence, or heat dissipation (Gorbunov & Falkowski,

https://doi.org/10.5194/egusphere-2026-1718
Preprint. Discussion started: 24 April 2026

2022). However, various photo-inactivating processes are activated action when electron generation exceeds the maximum capacity of the system. This response to high-light intensities is also a characteristic response of phytoplankton (Campbell & Serôdio, 2020; Zuo, 2025). Photo-damage is compensated by a continuous repair of the photosystem, and the outcome of these two opposing processes determines the resulting photo-inactivation or photoinhibition (Campbell and Tyysthärvi, 2012). The term photoinhibition (PI) is used generally to refer to any reduction in photosynthetic activity in response to exposure to excess light. More specifically, however, it is used to describe the situation where light induces a damage rate of the photosynthetic apparatus that exceeds the repair rate in the cell. This causes a reduction of the water-splitting process and the associated electron transport rate in the light-harvesting photosystem II (PSII) in the photosynthetic apparatus. Hence, the impact from PI limits the photosynthetic activity in the cells. The phenomenon has previously been described in field and laboratory studies of plants (e.g., Genty et al., 1989; Leverens et al., 1990) and phytoplankton (Kok, 1956; Platt et al., 1980; Long et al., 1994; Behrenfeld et al., 1998). Here, we apply the term, PI, to describe the reduction of functional reaction centers in PS II.

The distribution of photosynthetic activity in the euphotic zone has not been easily detectable from direct measurements of phytoplankton assemblages collected *in situ* in larger oceanic areas. Thus, it is poorly understood to what degree PI in natural communities is affecting photosynthetic activity. With the development of Single Turnover Active Fluorometry (STAF) and Fast Repetition Rate Fluorometry (FRRF) instrumentation designed for field studies (Schuback et al., 2024), the means for interrogating phytoplankton communities with respect to their PI status is now readily available. Variable fluorescence normalized to maximal fluorescence, F_v/F_m (Kolber et al., 1998), provides the photochemical quantum yield from the electron transport in PSII (Gorbunov and Falkowski, 2022). Hence, F_v/F_m can be used as an indicator of PSII status. Taxonomy and other factors influence the absolute values of F_v/F_m recorded. Nevertheless, one can assume that an increase in F_v/F_m in any given sample is indicative of an increase in the capacity for electron transport in PSII in that sample. Hence, changes in variable fluorescence may indicate photosynthetic response to changes in environmental variables as excess light (Behrenfeld et al., 1998; Oliver et al., 2003), nutrient availability (Beardall et al., 2001; Allakhverdiev and Murata, 2004), or trace metal availability (Lin et al., 2017; Schuback and Tortell, 2019; Gorbunov and Falkowski, 2022). From et al. (2014) applied this sensitivity of F_v/F_m to light and nutrient availability to develop a method for quantifying the impact of photoinhibition on phytoplankton samples.

From et al. (2014) sampled both laboratory cultures and natural marine phytoplankton populations for F_v/F_m taken from different light regimes. After sampling, they incubated the samples in either darkness or low light for up to 4 hours. No change in F_v/F_m was noted in the dark incubated samples. However, those incubated in low light often exhibited higher F_v/F_m after incubation than at the time of the original sampling. These findings were interpreted as implying that energy was required for the cells to repair photodamage in PSII. This has also been shown in laboratory studies (Allakhverdiev and Murata, 2004; Campbell & Serôdio 2020). Assuming this to be the case, the difference in F_v/F_m measured initially at the time of sampling and that determined after incubation of the sample in low light can be assumed to relate to repair of the damaged

https://doi.org/10.5194/egusphere-2026-1718
Preprint. Discussion started: 24 April 2026

photosynthetic apparatus and, thus, to the degree of PI experienced by a given phytoplankton community at the time of sampling.

Here, we extend the analysis of From et al. (2014) to natural communities in the euphotic zone of the North Atlantic. We analyse PI from a large data set, including a time-series station, collected in the temperate North Sea and evaluate the impact from light, nutrients, and other environmental variables in a principal component analysis (PCA). Based on this analysis, the correlation between light climate and PI is further explored by considering the light history experienced by phytoplankton cells at different depth levels and different times of the day. We then develop a statistical model constrained by data that describes PI as a function of photosynthetically available radiation (PAR) at the sampling depth. The model was tested against data from the subpolar and subtropical northern Atlantic. Finally, we discuss the presence of PI in the water column at three locations in the North Atlantic and its implications for photosynthesis and phytoplankton diversity.

2 Methods

2.1 Study area

Data were collected in the subpolar waters in the North Atlantic (~67°N), the North Sea (~57°N), and the subtropical Sargasso Sea (~30°N; Fig. 1, Table S1). The northeastern North Sea was visited during the period 16 - 30 July, 2016 (R/V Dana, National Institute of Aquatic Sciences, Technical University of Denmark) where F_v/F_m and low-light incubations for PI were measured at 127 stations, including a timeseries station with hourly low-light incubations over 36 hours (Fig. 1). Data from the subpolar North Atlantic were collected on board the Icelandic research vessel, Arní Fridriksson, in the period 17-19 June, 2021, where F_v/F_m determinations and low-light incubations were made at 3 stations at multiple depths, including a time-series station with a duration of 28 hours. Data from the Sargasso Sea were also collected on board R/V Dana in the period 11-20 April, 2014, where F_v/F_m and low-light incubations were determined at 10 m at 22 stations.

2.2 Hydrography, water sampling and turbulence measurements

Hydrographic data of conductivity, temperature, and depth (CTD) were on all three cruises determined with a Seabird SBE911 plus system. In the North Sea and Sargasso Sea, the rosettes were equipped with a Seabird SBE43 sensor, a SCUFA (self-contained underwater fluorescence apparatus) fluorometer and 12 10-liter Niskin bottles. In the Irminger Sea, the rosette was equipped with an oxygen SBE43 sensor, a LI-COR Biospherical PAR sensor, a Seapoint fluorometer (Seapoint Sensors Inc., USA) and 11 5-liter Niskin bottles.

Micro-scale turbulence was measured with a loose-tethered free-fall Rockland Scientific International (RSI) VMP-250 microstructure vertical profiler equipped with two shear probes. The vertical turbulent diffusion coefficient (k_v) was estimated from the dissipation rate of TKE (Osborn, 1980) assuming a constant mixing rate and following the procedure described in Bendtsen and Richardson (2018).

https://doi.org/10.5194/egusphere-2026-1718
Preprint. Discussion started: 24 April 2026

2.3 Nutrients and chlorophyll *a*

Water samples from the North Sea and Irminger Sea were tapped and immediately frozen for nutrient determination. The samples were analysed at Aarhus University, Department of Bioscience. Here, they were thawed, filtered (Milipore Millex-GP Hydrophylic PES 0.22 µm), and analysed by wet chemistry methods according to Grashoff et al. (1983). Nutrient determinations of the water samples from the Sargasso Sea were carried out as for the North Sea samples and measured using a SanPlus System Scalar auto analyser at Aarhus University, Denmark.

Chlorophyll *a* measurements were made fluorometrically (Arar & Collins, 1997) following ethanol (96%) extraction of chlorophyll retained on a glass fiber filter (Whatman). These were used to calibrate CTD fluorescence. Distributions of chlorophyll *a* and nutrients from the VERMIX study were previously analysed in Bendtsen and Richardson (2018).

2.4 Photosynthetically available radiation

The underwater light field of *in situ* photosynthetically available radiation (PAR) was measured by a PAR-sensor (Biospherical cosine QCP) mounted on the rosette. Generally, observations were made with the rosette deployed towards the sun. However, shading from the ship may still have impacted light at the uppermost samples taken at 5 m. The observed *in situ* PAR was applied in the PCA and linear regression analyses.

Surface PAR (S_{PAR}) was measured continuously by a Biospherical scalar QSR-2200 mounted on the ship and was used for analysing the impact of the light history of the water samples. The corresponding underwater light history (LH) was then estimated from the surface PAR following Beers law; $LH(d, \tau_0) = \alpha\, S_{PAR}(\tau_0) \exp(-d\, k_d)$, where α represents the reduction of light due to surface albedo, $S_{PAR}(\tau_0)$ represents the average S_{PAR} during a period, τ_0, prior to the time of sampling. The light attenuation coefficient, (k_d), describes the distribution of light with depth (d). The average light attenuation coefficient (k_d) in the North Sea during the cruise was 0.14 m^{-1} (Bendtsen & Richardson 2018). The value of α was assumed to be constant in the area and, therefore, to have no impact on the correlation analysis between PI and LH.

2.5 Low-light incubations

The degree of PI experienced by phytoplankton under natural conditions was assessed using STAF and FRRF to determine F_v/F_m from the upper 60 m in the North Sea (using FRRF) and Irminger Sea (STAF), and from 10 m depth in the Sargasso Sea (FRRF). Initial F_v/F_m determination following sample collection was made following dark incubation for a minimum of 30 min (From et al., 2014). The samples were thereafter incubated at low light (~50 µE m^{-2} s^{-1}) for 4 hours ± ~10 min, to eliminate PI. F_v/F_m was then again determined. The post-incubation F_v/F_m -value after 4 hours is referred to as corrected $F_v/F_m|^c$. The low-light incubations generally resulted in a higher $F_v/F_m|^c$ compared to the initial F_v/F_m, presumably due to repair of the photosynthetic apparatus supported by energy from the low photon flux. The impact from PI (i.e., $\Delta F_v/F_m$) was calculated as:

$$\Delta F_v/F_m = F_v/F_m|^c - F_v/F_m \quad (1)$$

https://doi.org/10.5194/egusphere-2026-1718
Preprint. Discussion started: 24 April 2026

Thus, the relative reduction of the maximum photochemical yield due to PI (Π_{PI}) could then be calculated:

$$\Pi_{PI} = (\Delta F_v/F_m)/(F_v/F_m|^c) \quad (2)$$

F_v/F_m data from the North Sea were measured with a FastOcean FRRf 3 sensor (Chelsea Technologies Group, UK) with a dark chamber installed, and the data were acquired in the FASTpro 8 software. The FastOcean FRRf 3 sensor had a detection limit of F_v/F_m = 0.150, and all values below this limit were noted as 0.150. The F_v/F_m data from the Irminger Sea were determined using a LABSTAF instrument (Oxborough, 2021). F_v/F_m data from the Sargasso Sea were determined using a FASTTRACKA fluorometer (Chelsea Instruments Group Ltd) (Richardson & Bendtsen 2017).

2.6 Analysis of PI

Photoinhibition, $\Delta F_v/F_m$, was analysed in relation to the light history as experienced by phytoplankton cells in the water column. Hence, the average light intensities of the 0-50 minutes and 1-6 hours prior to sampling of phytoplankton were determined. The instantaneous and average light intensities prior to sampling were calculated with respect to bottle closure time at each depth level. The correlations between photoinhibition and instantaneous and average light conditions prior to sampling were determined from a linear regression. The data analysis only considered data points with instantaneous PAR higher than 50 µE m^{-2} s^{-1} (discussed in section 3.1). The statistical software RStudio version 4.3.2 was used for the analysis (R Core Team 2021). Confidence levels for all statistical tests were set at a p-value < 0.05.

3 Results

3.1 Timeseries observations in the North Sea

A 36-hour long timeseries station was monitored between 29-30 July (referred to as day 211 and 212, respectively) above the shelf edge in the north-eastern North Sea (Fig. 1a), where water samples, CTD-casts, and turbulent shear measurements were collected every hour, except for short intervals during the night. Water mass distributions and dynamic conditions were relatively stable during the period. The surface mixed layer was about 10 m deep and characterized by temperatures above 16 °C, and with vertical turbulent diffusion coefficients ranging between ~10^{-2}- 0^{-3} m^2 s^{-1} (Fig. 2). Note that vertical mixing in the upper ~5 m could be influenced by disturbances from the free-drifting ship (draught of 5.7 m), and mixing rates obtained near the surface are, therefore, considered as an upper limit. Below the seasonal thermocline and in the depth range of 20-40 m, the temperature was ~8-12 °C and associated with relatively low values of the turbulent diffusion coefficients (< 10^{-5} m^2 s^{-1}).

The mixed layer concentration of chlorophyll *a* was, in general, very low (< 0.2 µg l^{-1}) whereas concentrations above 1 µg l^{-1} were observed in a subsurface chlorophyll *a* maximum at ~30 m depth (Fig. 3). Surface insolation of PAR (S_{PAR}) varied between cloud-free and cloudy conditions with more cloudy periods during the first day (Fig. 3a). The largest Π_{PI} was observed at the surface around midday during day 212. Below 20 m, there were only minor changes in Π_{PI} during the period.

https://doi.org/10.5194/egusphere-2026-1718
Preprint. Discussion started: 24 April 2026

The corrected variable fluorescence ($F_v/F_m|^c$) showed relatively minor changes during the day at all depth levels (Fig. 3c) whereas the lowest values of F_v/F_m were seen near the surface around midday. Short term variability along the shelf edge was also observed, e.g., co-variation between high chlorophyll *a* and F_v/F_m at 40 m depth the first day in the afternoon, i.e. at day 211.75.

Further analysis of the timeseries of Π_{PI} in the upper 20 m showed that maximum PI at all three depth levels occurred during midday (Fig. 4). Π_{PI} increased by 49%, 31%, and 21% at 5, 10, and 20 m depth, respectively. In general, Π_{PI} increased from sunrise to midday and decreased thereafter to zero by late afternoon. F_v/F_m varied in an inverse pattern, where a minimum value was observed around midday. Linear regressions of $F_v/F_m|^c$ versus time during the daylight hours showed a significant ($p < 10^{-3}$) decrease on day 212 at the three depth levels (R^2 ranging between 0.63 -0.79) and with the largest decrease (-0.008 h^{-1}) being seen at 5 m depth, corresponding to a drop of ~0.1 during the day. On day 211, the decrease was not significant except at 20 m depth (-0.004 h^{-1}, $R^2 = 0.40$, $p = 0.02$). The average surface insolation (S_{PAR}) during daytime on days 211 and 212 was 773 and 1856 µE m^{-2} s^{-1}, respectively. Variability of surface salinity (Fig. 4a) was associated the half-daily tidal motion (Bendtsen and Richardson, 2020) and was not correlated to S_{PAR}.

3.2 Low-light incubations in the North Sea

In addition to the time series station, water sampling for low light incubations in the North Sea was also carried out along 4 transects between sunrise and sunset, with sampling being approximately equally distributed during the day (Fig. 1a). The relative change in PI showed a similar pattern as found at the timeseries station, where the greatest PI was generally found in the nutrient depleted surface layer and above the subsurface chlorophyll *a* maximum (Fig. 5). The greatest values of PI were seen above the shallow areas on transect 5 (Fig. 5d). However, spatial variability of PI was observed both along the transects and with depth.

A PCA determined the relation between normalized environmental variables in the area, and variability in PI was analysed in relation to PC1 and PC2, explaining 45% and 19% of the variability, respectively (Fig. 6). The primary component explaining variability in the data set was associated with variability in temperature, i.e., related to the vertical separation of the surface and subsurface layer by the seasonal thermocline. *In situ* PAR and PI were tightly correlated and covaried with temperature, i.e., increased light and PI towards the warmer surface waters. Salinity was mainly anti-correlated with temperature and reflected the general salinity increase in the subsurface water masses. The anti-correlation between PAR and fluorescence (i.e., chlorophyll *a*) could be explained by the low surface concentration of chlorophyll and the attenuation of light by the relatively large chlorophyll *a* concentrations in waters below ~20 m depth. Nutrients were anti-correlated with both temperature and fluorescence due to the nutrient depletion and biological uptake in the surface layer. Thus, the PCA showed a strong correlation between *in situ* PAR and PI. This was in accordance with both the general temporal patterns observed at the time-series station and the spatial variability along the four transects. Therefore, the relation between these two variables was analysed further.

https://doi.org/10.5194/egusphere-2026-1718
Preprint. Discussion started: 24 April 2026

Observations of *in situ* PAR near the surface showed values up to ~1000 µE m^{-2} s^{-1} around midday, and incubations at 5 m depth showed a corresponding pronounced maximum reduction of photosynthetic activity with $\Delta F_v/F_m$ values up to ~0.2 for samples collected between 12–14h in the afternoon (Fig. 7). Values close to zero were measured just after sunrise and before sunset. Both positive and negative $\Delta F_v/F_m$ values were found at deeper depths, i.e., with low ambient *in situ* PAR-values. Thus, the low-light incubations had no significant effect on the photosynthetic activity on samples already exposed to low light levels *in situ*. Part of this variation might be due to the relatively weak incubation light of ~50 µE m^{-2} s^{-1} inducing PI in cells acclimated to an even lower light level near the bottom of the euphotic zone. Samples collected from ambient *in situ* light levels below 50 µE m^{-2} s^{-1} were, therefore, excluded from the subsequent analysis of PI.

Distributions of $\Delta F_v/F_m$ and Π_{PI} from the VERMIX-cruise showed a corresponding increase with *in situ* PAR (Fig. 8). A statistical PI-model could then be constructed based on a linear regression of all North Sea incubation data of Π_{PI} and *in situ* PAR > 50 µE m^{-2} s^{-1} (Fig. 8b):

$$\Pi_{PI} = \pi_a PAR + \pi_b \quad (3)$$

where $\pi_a = 3.76 \cdot 10^{-4}$ (µE m^{-2} s^{-1})$^{-1}$ and $\pi_b = 0.078$. The Π_{PI}-model of PI resulted in a $R^2 = 0.40$ ($p < 10^{-3}$, n = 281). Thus, the PI-model implies that the photochemical yield is reduced by ~45% for PAR-levels at ~1000 µE m^{-2} s^{-1} (i.e., 0.376+0.078). The offset (π_b) presumably reflects uncertainties associated with the experimental procedures as well as other factors/processes than light which influence photosynthetic activity. A similar significant regression model was also determined for $\Delta F_v/F_m$ with a slope and intercept of $1.38 \cdot 10^{-4}$ and 0.038 ($p < 10^{-3}$, R^2=0.37), respectively (Fig. 8a).

3.3 Impact of light history on PI

PI was analysed in relation to the light history experienced by the water sample. The light history (LH) was estimated from variations in surface PAR in a period (τ) prior to the sampling time (τ_0), i.e., when the Niskin bottle was closed. The potential role of the accumulated photon flux experienced over a period of time (τ) prior to τ_0 was examined in a statistical correlation analysis of Π_{PI} versus the light history providing a linear regression model similar to Eq. 3. The light history, determined as the average S_{PAR} during the period τ was calculated for a range of τ-values in time intervals from 10 minutes and up to 6 hours before the bottle was closed (Table 1).

The proportion of variation explained by the linear regression when the light history was averaged 10 and 20 minutes before the water sampling resulted in a similar or slightly larger R^2 (0.40-0.41) than the PI-model based on the instantaneous light (Eq. 3). A similar statistic of R^2 was found for an analysis based on surface samples only (R^2 = 0.44-0.45). Using time intervals longer than 20-30 minutes before the water sampling, resulted in a gradual lowering of R^2, e.g., a time interval of 1 hour resulted in an R^2 of 0.36. Increasing the time period for averaging the PAR before bottle closure further yielded an increasingly poorer explanatory power of the linear regression (e.g., R^2 = 0.31 and 0.16 for time periods of τ = 2 and 6 hours, respectively).

Thus, the highest R^2 values were obtained in relationships based on light intensities averaged over a few tens of minutes before the sample was enclosed in darkness in the Niskin bottle. This suggests that the level of PI in natural phytoplankton

https://doi.org/10.5194/egusphere-2026-1718
Preprint. Discussion started: 24 April 2026

communities reaches a near-steady state within a relatively short time (i.e., $\tau \sim 20$ minutes) when exposed to a given light level during the day. Considering the small difference in the statistical models between the instantaneous and short time averaged *in situ* PAR, we simply applied the instantaneous light as being representative for the photon flux causing PI in the phytoplankton cells.

3.4 PI from subtropical to subpolar areas

Measurements from low-light incubations made in the Sargasso Sea and the Irminger Sea were analysed in relation to the statistical PI-model from the northern North Sea (Fig. 1b). The three areas covered conditions in the center of the oligotrophic subtropical gyre (Sargasso Sea), the relatively high-productive subpolar region in the North Atlantic (Irminger Sea), and the transition between shelf and slope water masses across the European shelf (North Sea). The average PI for light levels above 50 µE m^{-2} s^{-1} were 0.33±0.02 (SE, n = 11) and 0.21±0.05 (n = 12) for the Irminger Sea and the Sargasso Sea, respectively (Fig. 8). However, in comparison with the PI-model, the values of Π_{PI} tended to be larger in the Irminger Sea. Thus, the model underestimated the impact on potential photochemical yield from PI in this area. PI in the Sargasso Sea was also in general accordance with the PI-model, however with a tendency to be less than the PI-model for highest light levels. In general, Π_{PI} in the Irminger Sea and Sargasso Sea supported the PI-model showing a significant PI for high light levels. However, deviations from the model in both areas indicated that other processes than light also affect the relationship with *in situ* PAR.

4 Discussion

Photoinhibition in natural phytoplankton communities in the euphotic zone is shown here to significantly reduce photosynthetic capacity in the surface layer in all three areas. The short response time (< 30 min) for the onset of PI for a given light level that was found for the entire North Sea data set is in accordance with observational studies of the photochemical response to short-term increases in light exposure (Alderkamp et al., 2010) and the mechanistic modeling of PI based on laboratory experiments (Baklouti et al., 2006). However, the impact of PAR on a natural water sample is also influenced by vertical mixing. This has to be considered in relation to the estimated response time as the time spent at shallower depth levels during a short period of time due to mixing would tend to increase the amount of PAR received (Oliver et al., 2003; Ross et al., 2011). We analysed the potential influence of mixing on the PI recorded here from the observed turbulence. A representative time scale (τ) for vertical displacements (Δz) could be estimated from the vertical turbulent diffusion coefficient (k_v): $\tau \sim \Delta z^2/k_v$. The vertical turbulent diffusion coefficient near the surface was estimated to be in the range ~10^{-2}-10^{-3} m^2 s^{-1} (Fig. 2b), so vertical displacements of ~5 m in this layer then correspond to turbulent diffusive timescales of 0.7-7 hours. Thus, the typical vertical movement due to turbulent motion during periods of less than an hour could have exposed some of the 5 m samples to light at the surface, i.e., an increase in PAR of ~50%. Turbulent motion can, therefore, explain some of the variability of Π_{PI} to PAR in samples near the surface. Turbulent motion below10

https://doi.org/10.5194/egusphere-2026-1718
Preprint. Discussion started: 24 April 2026

m depth ($k_v < 10^{-3}$ m^2 s^{-1}) implied timescales longer than 7 hours and would, therefore, have had minor effects on variations in PAR exposure during the day. Other environmental factors, e.g. temperature (Long et al., 1994) and nutrient availability (Sugget et al., 2009), may also affect PI and explain some of the variability of the data in comparison with the statistical PI-model. However, the strong correlation between PI and PAR identified from the PCA supported that light exposure was the dominating variable explaining variability in PI.

The PI-model presented here does not include transient effects due to time lags between the damage and repair cycles of PSII (He and Chow, 2003; From et al., 2014) where the potential asymmetric response due to gradual damage and repair of the photosynthetic apparatus during the daily insolation cycle may imply a different PI response before and after noon. The approximately symmetrical response of PI around midday (Fig. 4, 6) indicated that photo-damage over the entire day was in a quasi-stationary balance with repair processes in the cells, i.e., the characteristic timescale of repair processes was comparable to the variations in PI. Thus, because of the symmetrical PI around midday and the relatively high correlation with instantaneous light, we consider the impact from an asymmetrical response between damage and repair as a second-order effect.

Sampling at the time-series station is only a proxy for the temporal variation of the phytoplankton cells because of advective transport due to ocean currents. Thus, some of the variation could also potentially be explained by changed conditions upstream of the sampling sites (Bendtsen and Richardson, 2020; Cordier et al, 2025). Nevertheless, similarities in the evolution of Π_{PI} and F_v/F_m at the time-series station on the two days of sampling indicate a common temporal pattern with an extremum around midday. The time-series station at the shelf edge in the northern North Sea showed a significant PI during the day in the upper ~20 m (Fig. 4). PI in the upper 5 m was found to increase and exceed 30% towards midday. PI decreased in the afternoon and during the night. This sensitivity was also reflected in the daily variation of insolation due to cloud cover, where the relatively low insolation during the first day in the time-series resulted in lower PI at midday (i.e., day 211.5) than observed on the following day when insolation was greater (Fig. 3b). This correlation between PI and light was in accordance with the PCA (Fig. 6) based on all data from the area (Fig. 5).

4.1 Impact on phytoplankton communities and primary production estimates

It is generally assumed that optimal conditions for phytoplankton photosynthesis are found at the ocean surface, i.e., where light is most available. Data presented here, however, suggest this may not be the case as phytoplankton communities in the three study regions of the North Atlantic all regularly experienced PI in the upper 10 m or more of the water column. As these regions represent vastly different ecosystem types, the consistent finding of PI suggests that photosynthesis in the surface waters of much of the global ocean may be constrained by PI. While this result may, at first, appear counterintuitive, we suggest that it might be explained through physical and/or evolutionary considerations.

As light is attenuated exponentially with depth, a phytoplankter with a photosynthetic apparatus that performs optimally at low light will be able to thrive over a greater percentage of the water column than one whose apparatus performs optimally at high light. Another consideration could be that Earth conditions, including the global ocean light climate, have varied

https://doi.org/10.5194/egusphere-2026-1718
Preprint. Discussion started: 24 April 2026

dramatically in the over 3 billion years since photosynthesis emerged, due to gradual increases of insolation, changing ocean chemistry, variations in cloud cover, and atmospheric composition. It is not hard to imagine that, in periods with less light available at the ocean surface than today, conditions optimal for phytoplankton photosynthesis may have been found at the ocean surface and, indeed, that the potential to adjust the vertical distribution of optimal photosynthetic performance has provided the global phytoplankton community with resilience and the ability to optimize its photosynthetic performance in the face of varying light conditions.

The ubiquitous occurrence of photoinhibition in the surface layer of the ocean demonstrated here has implications for estimating global ocean production in that such estimates are highly dependent on the photosynthetic parameters used in the models applied (Neale and Thomas, 2017; Richardson and Bendtsen, 2019). A survey (Richardson et al., 2016) of reported values for photosynthetic parameters from natural communities relevant for estimating primary production indicated large variability in parameter values. Based on the results reported here, at least some of that variability seems likely to derive from differences in the ambient light conditions when the photosynthetic measurements were made. The effect of photoinhibition on photosynthetic parameters may potentially be minimized by conducting incubation experiments for the determination of these parameters either early or late in the day. In any case, it would be advisable that the ambient light intensity at the sample depth be recorded and reported when presenting results of primary production estimates for natural phytoplankton communities. That PI apparently reduces photosynthetic activity (Π_{PI}) in the upper ocean today impacts not only the potential photosynthesis in this layer, as shown here, but also community composition, as different phytoplankton groups and species show different affinities for light climate (Richardson et al., 1983). The highest concentrations of chlorophyll in the water column in all regions were found below the surface layer. i.e., in the deep chlorophyll maximum (DCM). That these DCMs were located at depth levels below the depth to which PI was estimated to penetrate suggests that PI may also be a determinant of the vertical distribution of phytoplankton.

5 Conclusion

Natural phytoplankton communities experienced PI over much of the day in water samples from subpolar, temperate, and subtropical regions in the North Atlantic. PI was found to mainly respond to changes in solar insolation within 30 minutes. A linear regression model of PI versus *in situ* PAR showed a significant reduction of the maximum photochemical yield due to the intensity of solar insolation. Data from subtropical and subpolar areas were consistent with the statistical model, and model simulations of the daily PI showed a reduction between 10-30% of the maximum photosynthetic efficiency of PSII in all areas. These results show the dynamic short-time response of the photosynthetic system to changes in light and support that PI is a ubiquitous phenomenon in the upper ocean.

https://doi.org/10.5194/egusphere-2026-1718
Preprint. Discussion started: 24 April 2026

Code, data, or code and data availability

Incubation-, nutrient- and light-data are included in Supplementary Information.

Supplement link

Supplementary information is included.

Author contributions

KR planned the cruise and designed the experiments. KR, ND, and JB carried out measurements and collected water samples. JB, LD and KR wrote the manuscript draft. All authors reviewed and edited the manuscript.

Competing interests

The authors declare that they have no conflict of interest.

Acknowledgements

We thank the captain and crew on-board R/V Dana (R/V Dana, National Institute of Aquatic Sciences, Technical University of Denmark) for very helpful assistance and support during the cruises to the Sargasso Sea (2014) and the North Sea (2016). Similarly, we thank the captain and crew on the Icelandic research vessel, Arní Fridriksson (Marine and Freshwater Research Institute, Iceland) for very helpful assistance during the cruise to the Irminger Sea and Denmark Strait in 2021.

Financial support

This study was supported by funding by the Danish Centre for Marine Research, the Villum Foundation and by a grant from the Carlsberg Foundation (H.M. Queen Margrethe's and Vigdís Finnbogadóttir´s Interdisciplinary Research Centre on Ocean, Climate, and Society, CF-20-0071).

Tables

Table 1 Statistical correlation analysis of Π_{pi} versus the Light history experienced over a time period (τ) prior to the water sampling, i.e., the closing of the Niskin bottle: Correlation coefficient (R^2), and the range of number of samples for the different light histories (n). Significant values ($p<0.001$) are marked (*).

https://doi.org/10.5194/egusphere-2026-1718
Preprint. Discussion started: 24 April 2026

Depth	All depths	0-10 m	>10 m
Time (τ)	R^2 (n=276:281)	R^2 (n=195:197)	R^2 (n=83:84)
0 min	0.40*	0.44*	0.03
10 min	0.41*	0.45*	0.03
20 min	0.40*	0.45*	0.03
30 min	0.39*	0.44*	0.03
1 hr	0.36*	0.40*	0.01
2 hrs	0.31*	0.33*	<0.01

Figure captions

Figure 1 Locations of stations with low light incubations (white circles), the timeseries station (white triangle), and stations with chlorophyll *a* measurements (bullets) from the VERMIX cruise in the North Sea. Colors show the sea surface temperature obtained from MODIS data, 16 July 2016. (b) Locations of incubation experiments (white circles) from the North Sea (1), the Sargasso Sea (2) and the Irminger Sea (3), and monthly averaged chlorophyll *a* in June 2021 (NASA Ocean Biology Processing Group, 2017).

Figure 2 Observations from the VERMIX-timeseries station between 29 July and 30 July (i.e., day 211 and 212, respectively; time of observations marked with gray dots). (a) Potential temperature (θ), and (b) Log_{10} of the vertical diffusion coefficient (k_v).

Figure 3 Observations from the VERMIX-timeseries station. (a) Photosynthetically available radiation at the surface (S_{PAR}), and distributions (colored circles) in the surface layer of (b) Π_{PI}, (c) $F_v/F_m|^c$ and (d) F_v/F_m. (b-d) Filled contours show observed chlorophyll *a*.

Figure 4 Observations from the VERMIX-timeseries station of (a) Surface salinity (black, practical salinity S_P) and photosynthetically available radiation at the surface (gray, S_{PAR}). Observations at three depth levels of (b) Π_{PI}, (c) $F_v/F_m|^c$ and (d) F_v/F_m.

Figure 5 Observations along the four VERMIX-transects of chlorophyll *a* (Chl) and relative change in F_v/F_m in low-light incubations (Π_{PI}).

Figure 6 Principal component analysis (PCA) of temperature (T), *in situ* light (PAR), PI determined from the relative change in F_v/F_m in low-light incubations, nitrate (NO3), phosphorus (PO4), silicate (Si), salinity (S) and fluorescence from

https://doi.org/10.5194/egusphere-2026-1718
Preprint. Discussion started: 24 April 2026

chlorophyll *a* (Flu). The first and second PC explained 44.9 and 18.9 % of the variance, respectively, and the relative contribution from the two PC's (cos2) are shown with colors.

Figure 7 VERMIX-observations of (a) *in situ* PAR, and (b) $\Delta F_v/F_m$ versus local time of day. Colors show observations from the upper 5 m (red) and below (blue).

Figure 8 (a) $\Delta F_v/F_m$ and (b) Π_{PI} versus *in situ* PAR from the VERMIX-cruise (red, bullets), the Irminger Sea (brown, squares) and Sargasso Sea (blue, diamonds). Linear regressions to the the VERMIX-observations (>50 µE m^{-2} s^{-1}) are shown as red lines.

References

Alderkamp, A.-C., de Baar, H. J. W., Wisser, R. J. W., and Arrigo, K. R.: Can photoinhibition control phytoplankton abundance in deeply mixed water columns of the Southern Ocean?, Limnol. Oceanogr., 55, 1248–1264, https://doi.org/10.4319/lo.2010.55.3.1248, 2010.

Allakhverdiev, S. I., and Murata, N.: Environmental stress inhibits the synthesis de novo of proteins involved in the photodamage–repair cycle of Photosystem II in *Synechocystis* sp. PCC 6803, Biochim. Biophys. Acta, 1657, 23–32, https://doi.org/10.1016/j.bbabio.2004.03.003, 2004.

Arar, E. J., and Collins, C. B.: In vitro determination of chlorophyll a and pheophytin in marine and freshwater algae by fluorescence, National Exposure Research Laboratory, U.S. Environmental Protection Agency, Cincinnati, Ohio, USA, 1997.

Baklouti, M., Diaz, F., Pinazo, C., Faure, V., Quéguiner, B.: Investigation of mechanistic formulations depicting phytoplankton dynamics for models of marine pelagic ecosystems and description of a new model, Progr. Oceanogr., 71, 34–58, https://doi.org/10.1016/j.pocean.2006.05.002, 2006.

Beardall, J., Youung, E., and Roberts, S.: Approaches for determining phytoplankton nutrient limitation, Aquatic Sci., 63, 43–69, https://doi.org/10. 1007/ PL00001344, 2001.

Behrenfeld, M. J., Prasil, O., Kolber, Z. S., Babin, M., and Falkowski, P. G.: Compensatory changes in Photosystem II electron turnover rates protect photosynthesis from photoinhibition, Photosynthesis Research, 58, 259–268, 1998.

Bendtsen, J., and Richardson, K.: Turbulence measurements suggest high rates of new production over the shelf edge in the north-eastern North Sea during summer, Biogeosciences, 15, 7315–7332, https://doi.org/10.5194/bg-15-7315-2018, 2018.

Bendtsen J., and Richardson K.: New production across the shelf-edge in the northeastern north sea during the stratified summer period, J. Mar. Syst., 211, 103414, 2020.

Bendtsen, J., Sørensen, L. L., Daugbjerg, Lundholm, N., and Richardson, K.: Phytoplankton diversity explained by connectivity across a mesoscale frontal system in the open ocean, Sci. Rep., 13, 12117, https://doi.org/10.1038/s41598-023-38831-1, 2023.

https://doi.org/10.5194/egusphere-2026-1718
Preprint. Discussion started: 24 April 2026

Campbell, D. A., and Tyystjärvi, E.: Parameterization of photosystem II photinactivation and repair, Biochim. Biophys. Acta, 1817, 258–265, https://doi.org/10.1016/j.bbabio.2011.04.010, 2012.

Campbell, D. A., and Serôdio, J.: Photoinhibition of photosystem II in phytoplankton: Processes and patterns, p. 329–365. In A. Larkum, A. Grossmann, and J. Raven [eds.], Photosynthesis in algae: Biochemical and physiological mechanisms, Advances in Photosynthesis and Respiration, 45, Springer, 2020.

Cordier, A., Bendtsen, J., Daugbjerg, N., From, N., Jónasdóttir, S. H., Mousing, E. A., Christensen, J. T., Silva, T., and Richardson, K.: Patchiness of plankton ecosystem structure due to nutrient mixing along the shelf edge in the North Sea, Sci. Rep., 15, 1183, https://doi.org/10.1038/s41598-024-83811-8, 2025.

From, N., Richardson, K., Mousing, E. A., Jensen, P. E.:Removing the light history signal from normalized variable fluorescence (F_v/F_m) measurements on marine phytoplankton, Limnol. Oceanogr. Methods, 12, 776–783, https://doi.org/10.4319/lom.2014.12.776, 2014.

Genty, B., Briantais, J.-M., and Baker, N. R.:The relationship between the quantum yield of photosynthetic electron-transport and quenching of chlorophyll fluorescence, Biochim. Biophys. Acta, 990, 87–92, 1989.

Gorbunov, M.Y., and Falkowski, P.G.: Using chlorophyll fluorescence to determine the fate of photons absorbed by phytoplankton in the world's oceans, Ann. Rev. Mar. Sci., 14, 213–238, https://doi.org/10.1146/annurev-marine-032621-122346, 2022.

Grasshoff, K., Ehrhardt, M., and Kremling, K.: Methods of seawater analysis, 2nd edn (Weinheim: Verlag Chemie), 1983.

He, J., and Chow, W.S.: The rate coefficient of repair of photosystem II after photoinactivation, Physiol. Plant, 118, 297–304, 2003.

Kok, B.: On the inhibition of photosynthesis by intense light, Biochimica et Biophysica Acta, 21, 234–244, 1956.

Kolber, Z.S., Prášil, O., and Falkowski, P.G.: Measurements of variable chlorophyll fluorescence using fast repetition rate techniques: defining methodology and experimental protocols, Biochim. Biophys. Acta, 1367, 88–106, 1998.

Leverenz, J. W., Falk, S., Pilstrôm, C.-M., and Samuelsson, G.: The effects of photoinhibition on the photosynthetic light-response curve of green plant cells (*Chlamydomonas reinhardtil*), Planta, 82, 161-168, 1990.

Lin, H., Kuzminov, F.I., Park, J., Lee, S., Falkowski, P. G., and Gorbunov, M. Y.: The Fate of Photons Absorbed by Phytoplankton in the Global Ocean, Science, 351, 264–267, https://doi.org/10.1126/science.aab2213, 2016.

Long, S.P., Humphries, S., and Falkowski, P.G.: Photoinhibition of photosynthesis in nature, Annu. Rev. Plant Physiol. Plant Mol. Biol., 45, 633–662, 1994.

NASA Ocean Biology Processing Group: MODIS-Aqua Level 3 Mapped Photosynthetically Available Radiation Data Version R2018.0 [Data set], NASA Ocean Biology DAAC, https://doi.org/10.5067/AQUA/MODIS/L3M/PAR/2018, 2017.

https://doi.org/10.5194/egusphere-2026-1718
Preprint. Discussion started: 24 April 2026

Neale, P. J., and Thomas, B. C.: Inhibition by ultraviolet and photosynthetically available radiation lowers model estimates of depth-integrated picophytoplankton photosynthesis: global predictions for *Prochlorococcus* and *Synechococcus*. Global Change Biology, 23, 293–306, https://doi.org/10.1111/gcb.13356, 2017.

Oliver, R. L, Whittington, J., Lorenz, Z., and Webster, I. T.: The influence of vertical mixing on the photoinhibition of variable chlorophyll a fluorescence and its inclusion in a model of phytoplankton photosynthesis, J. Plankton Res., 25, 1107-1129, https://doi.org/10.1093/plankt/25.9.1107, 2003.

Osborn, T.R.: Estimate of the local rate of vertical diffusion from dissipation measurements, J. Phys. Oceanogr., 10, 83–89, https://doi.org/10.1175/1520-0485(1980)010<0083:EOTLRO>2.0.CO;2, 2019.

Oxborough K (2021) LabSTAF and RunSTAF Handbook. (Doc No. 2408-014-HB |Issue B). West Molesey: Chelsea Technologies Ltd 98, https://doi.org/10.25607/OBP-1029, 1980.

Platt, T., Gallegos, C., and Harrison, W.: Photoinhibition of photosynthesis in natural assemblages of marine phytoplankton, J. Mar. Res., 38, 687–701, 1980.

Richardson, K., Beardall, J., and Raven, J.A.: Adaptation of unicellular algae to irradiance: an analysis of strategies. New Phytol., 93, 157−191, 1983.

Richardson, K., and Bendtsen, J.: Photosynthetic oxygen production in a warmer ocean: the Sargasso Sea as a case study. Phil Trans R Soc A, 375, 20160329, http://doi.org/10.1098/rsta.2016.0329, 2017.

Richardson, K., and Bendtsen, J.: Vertical distribution of phytoplankton and primary production in relation to nutricline depth in the open ocean, Mar. Ecol. Prog. Ser., 620, 33–46, https://doi.org/10.3354/meps12960, 2019.

Richardson, K., Bendtsen, J., Kragh, T., and Mousing, E.A. Constraining the distribution of photosynthetic parameters in the global ocean. Front. Mar. Sci., 3, 269, https://doi.org/10.3389/fmars.2016.00269, 2016.

Ross, O. N., Geider, R. J., Berdalet, E., Artigas, M. L., and Piera, J.: Modelling the effect of vertical mixing on bottle incubations for determining in situ phytoplankton dynamics. i. growth rates, Mar. Ecol. Prog. Ser., 435, 13–31. https://doi.org/10.3354/meps09193, 2011.

Schuback, N., and Tortell, P. D.: Diurnal regulation of photosynthetic light absorption, electron transport and carbon fixation in two contrasting oceanic environments, Biogeosciences, 16, 1381–1399, 2011, https://doi.org/10.5194/bg-16-1381-2019, 2019.

Schuback, N., Tortell, P. D., Berman-Frank, I., Campbell, D.A., Ciotti, A., Courtecuisse, E., Erickson, Z. K., Fujiki, T., Halsey, K., Hickman, A. E., Huot, Y., Gorbunov, M. Y., Hughes, D. J., Kolber, Z. S., Moore, C. M., Oxborough, K., Prášil, O., Robinson, C. M., Ryan-Keogh, T. J., Silsbe, G., Simis, S., Suggett, D. J., Thomalla, S., and Varkey D. R.: Single-Turnover variable chlorophyll fluorescence as a tool for assessing phytoplankton photosynthesis and primary productivity: opportunities, Caveats and Recommendations, Front. Mar. Sci., 8, 690607, https//doi.org/10.3389/fmars.2021.690607, 2021.

Sugget D. J., Moore C. M., Hickman A. E., and Geider R. J.: Interpretation of fast repetition rate (FRR) fluorescence: signatures of phytoplankton community structure vs. physiological state, Mar. Ecol. Prog. Ser., 376,1–19, https://doi.org/10.3354/meps07830, 2009.

https://doi.org/10.5194/egusphere-2026-1718
Preprint. Discussion started: 24 April 2026

Zuo, G.: Non-photochemical quenching (NPQ) in photoprotection: insights into NPQ levels required to avoid photoinactivation and photoinhibition, New Phytologist, 246, 1967–1974, https://doi.org/10.1111/nph.70121, 2025.

https://doi.org/10.5194/egusphere-2026-1718
Preprint. Discussion started: 24 April 2026

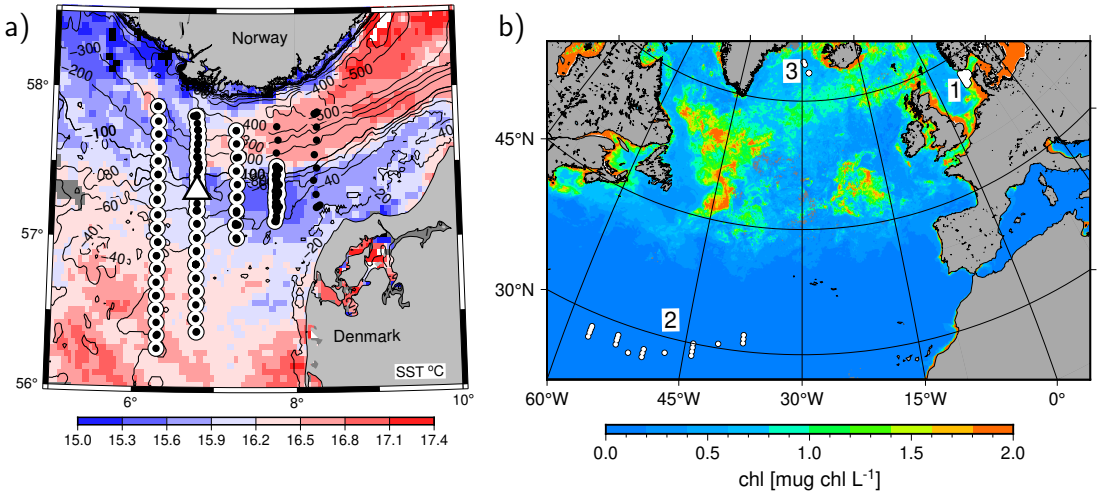

Figure 1 (a) Locations of stations with low light incubations (white circles), the timeseries station (white triangle), and stations with chlorophyll a measurements (bullets) from the VERMIX cruise in the North Sea. Colors show the sea surface temperature obtained from MODIS data, 16 July 2016. (b) Locations of incubation experiments (white circles) from the North Sea (1), the Sargasso Sea (2) and the Irminger Sea (3), and monthly averaged chlorophyll a in June 2021 (NASA Ocean Biology Processing Group, 2017).

https://doi.org/10.5194/egusphere-2026-1718
Preprint. Discussion started: 24 April 2026

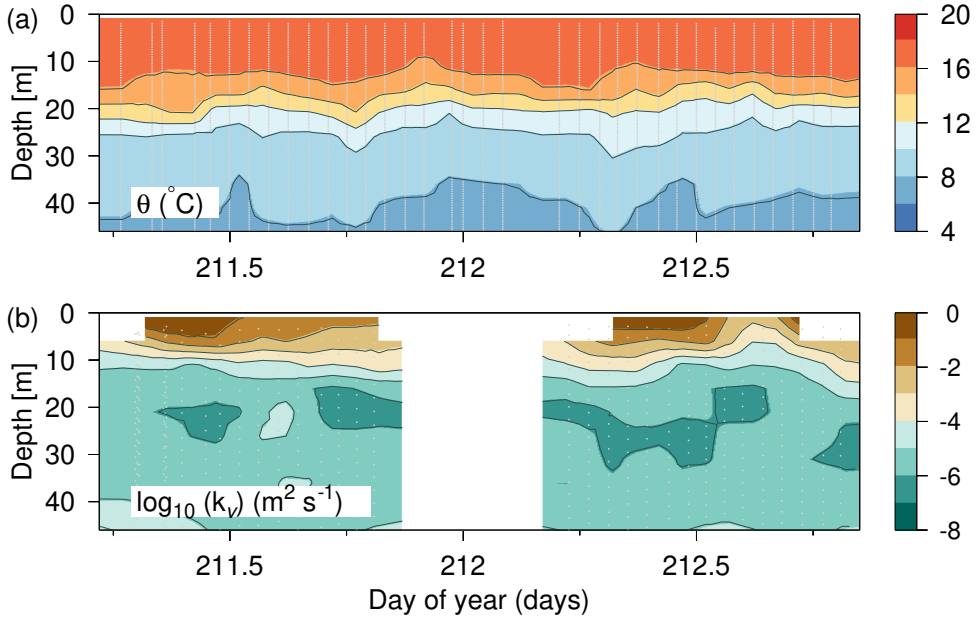

Figure 2 Observations from the VERMIX-timeseries station between 29 July and 30 July (i.e., day 211 and 212, respectively; time of observations marked with gray dots). (a) Potential temperature (θ), and (b) Log_{10} of the vertical diffusion coefficient (k_v).

https://doi.org/10.5194/egusphere-2026-1718
Preprint. Discussion started: 24 April 2026

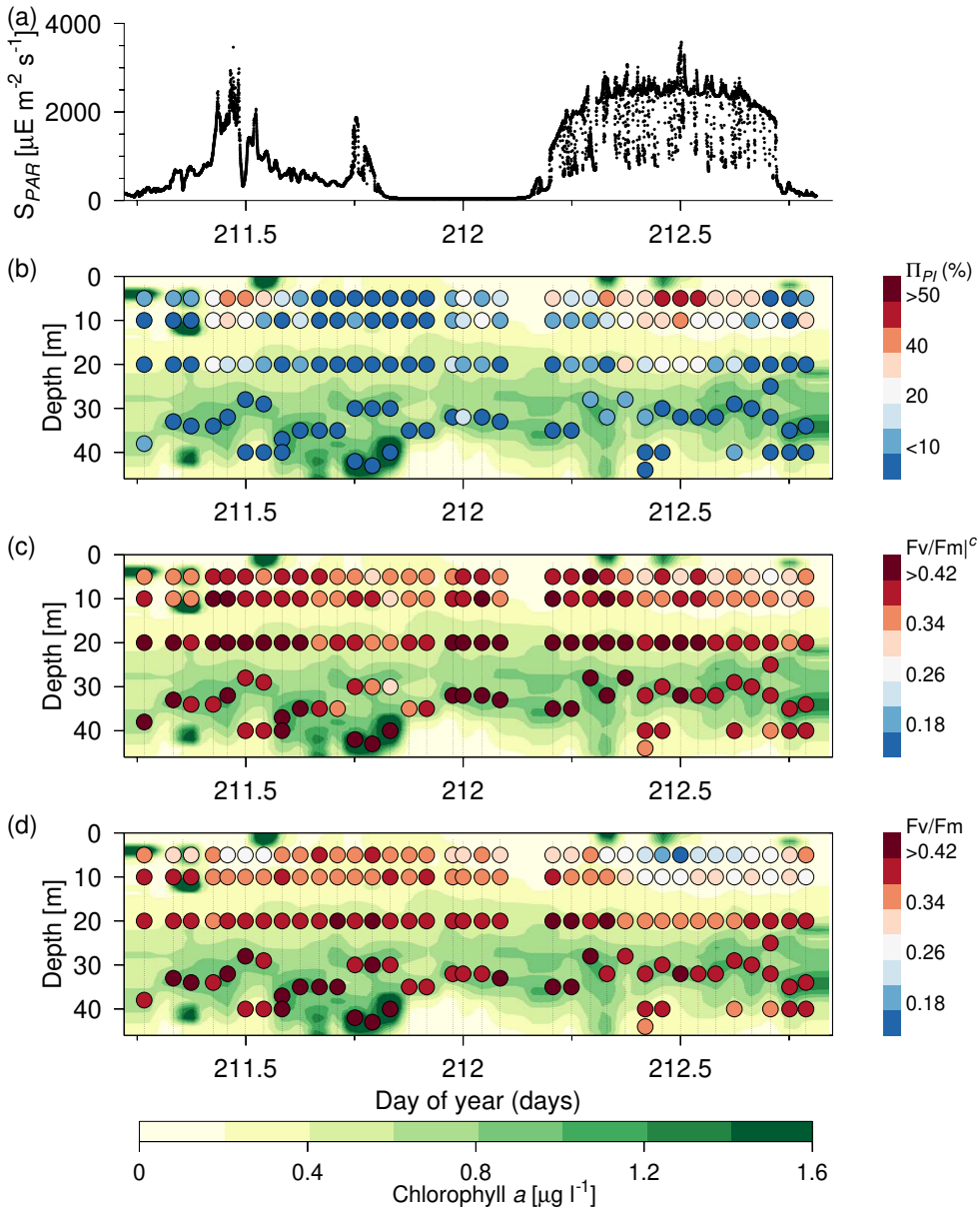

Figure 3 Observations from the VERMIX-timeseries station. (a) Photosynthetically available radiation at the surface (S_{PAR}), and distributions (colored circles) in the surface layer of (b) Π_{PI}, (c) $F_v/F_m|^c$ and (d) F_v/F_m. (b-d) Filled contours show observed chlorophyll *a*.

https://doi.org/10.5194/egusphere-2026-1718
Preprint. Discussion started: 24 April 2026

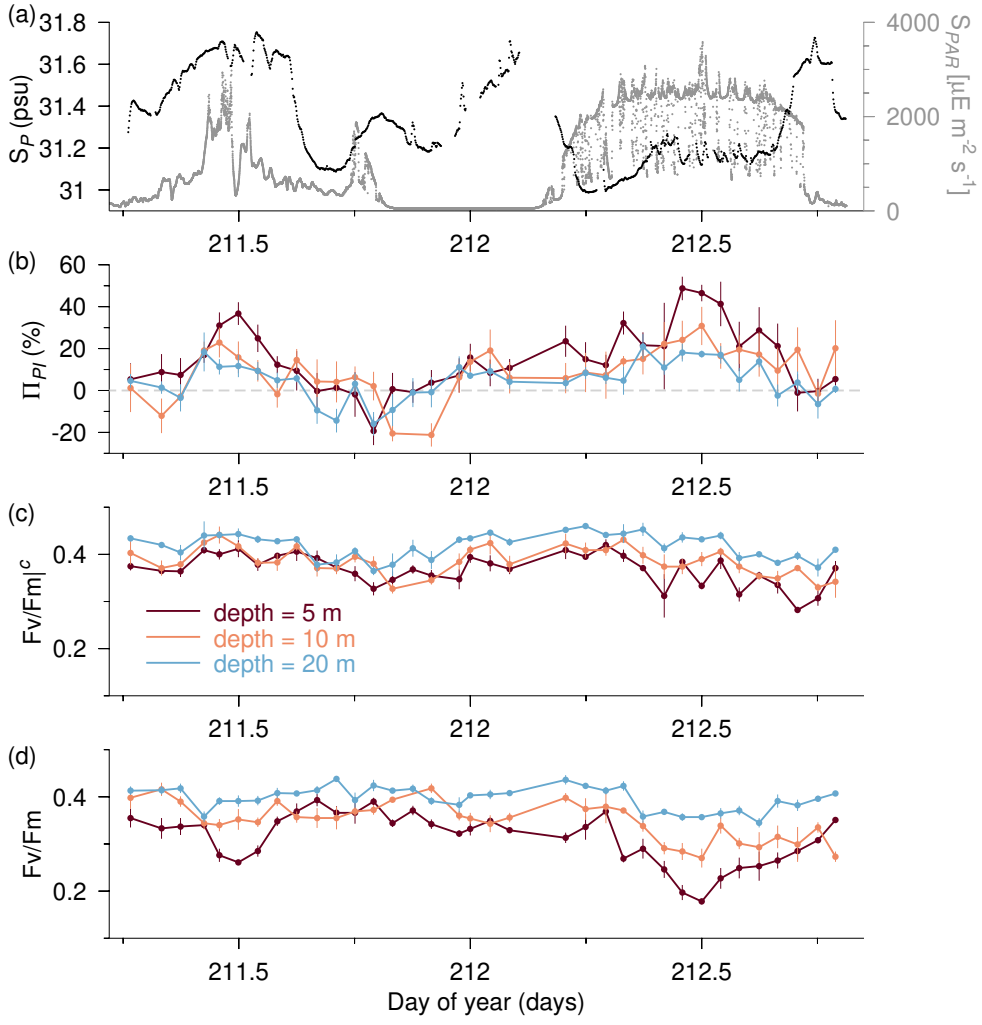

Figure 4 Observations from the VERMIX-timeseries station of (a) Surface salinity (black, practical salinity S_P) and photosynthetically available radiation at the surface (gray, S_{PAR}). Observations at three depth levels of (b) Π_{NPQ}, (c) $F_v/F_m|^c$ and (d) F_v/F_m.

https://doi.org/10.5194/egusphere-2026-1718
Preprint. Discussion started: 24 April 2026

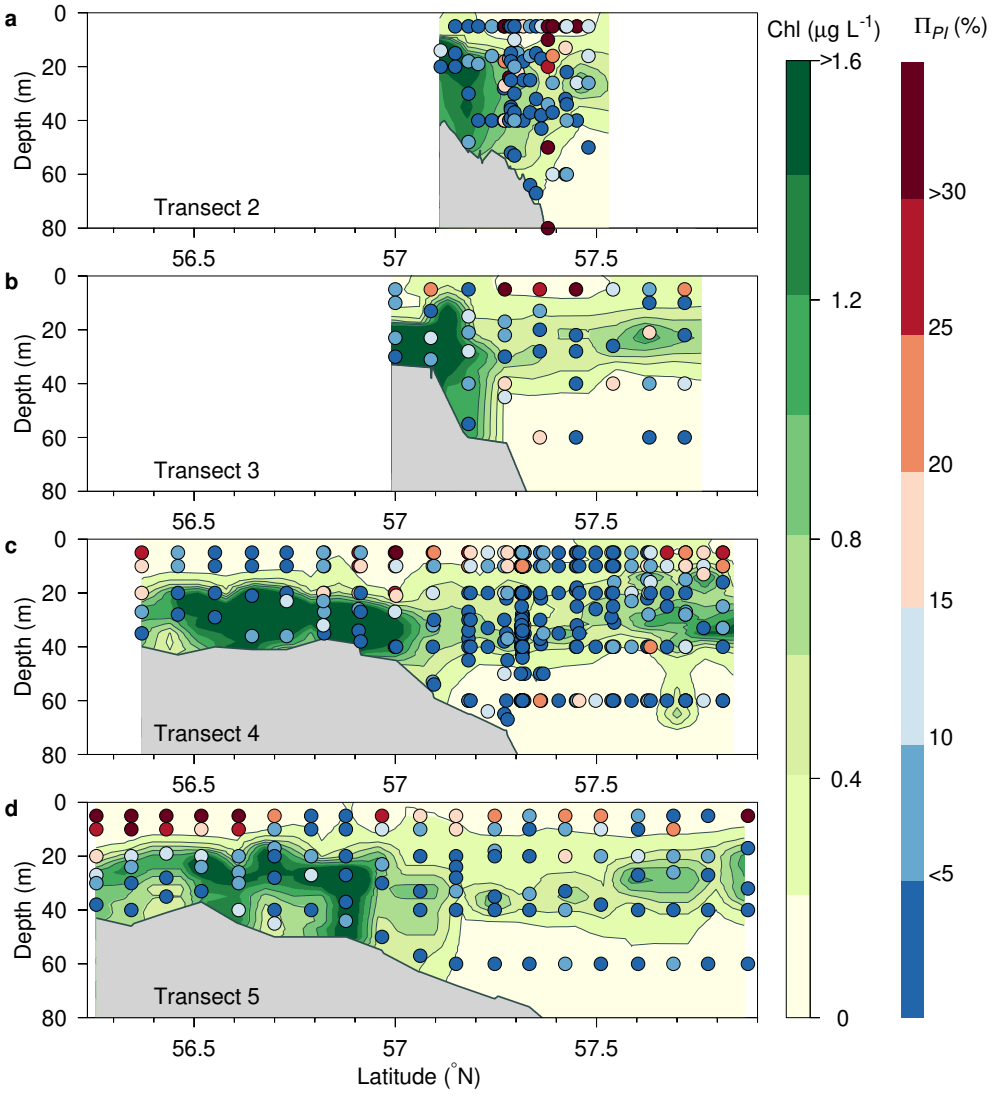

Figure 5 Observations along the four VERMIX-transect of chlorophyll a and relative change in F_v/F_m in low-light incubations (Π_{NPQ}).

https://doi.org/10.5194/egusphere-2026-1718
Preprint. Discussion started: 24 April 2026

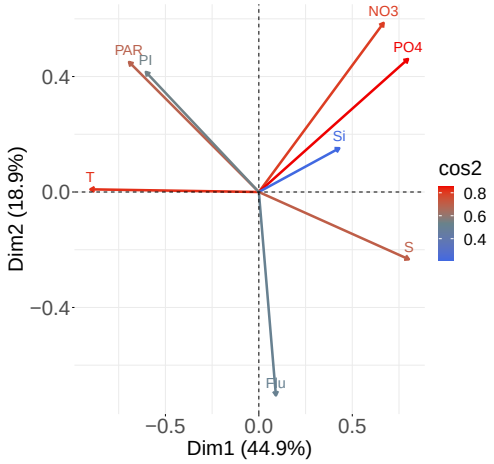

Figure 6 Principal component analysis (PCA) of temperature (T), *in situ* light (PAR), PI determined from the relative change in F_v/F_m in low-light incubations, nitrate (NO3), phosphorus (PO4), silicate (Si), salinity (S) and fluorescence from chlorophyll *a* (Flu). The first and second PC explained 44.9 and 18.9 % of the variance, respectively, and the relative contribution from the two PC's (cos2) are shown with colors.

https://doi.org/10.5194/egusphere-2026-1718
Preprint. Discussion started: 24 April 2026

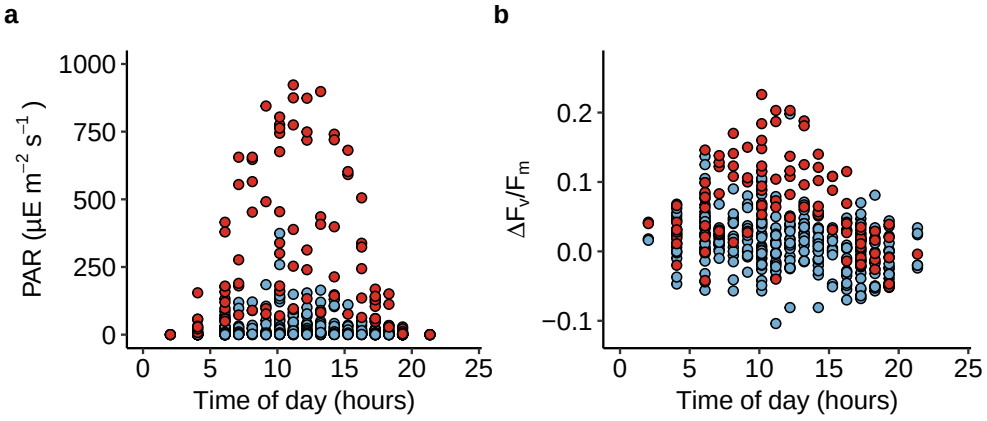

Figure 7 VERMIX-observations of (a) *in situ* PAR, and (b) $\Delta F_v/F_m$ versus local time of the day. Colors show observations from the upper 5 m (red) and below (blue).

https://doi.org/10.5194/egusphere-2026-1718
Preprint. Discussion started: 24 April 2026

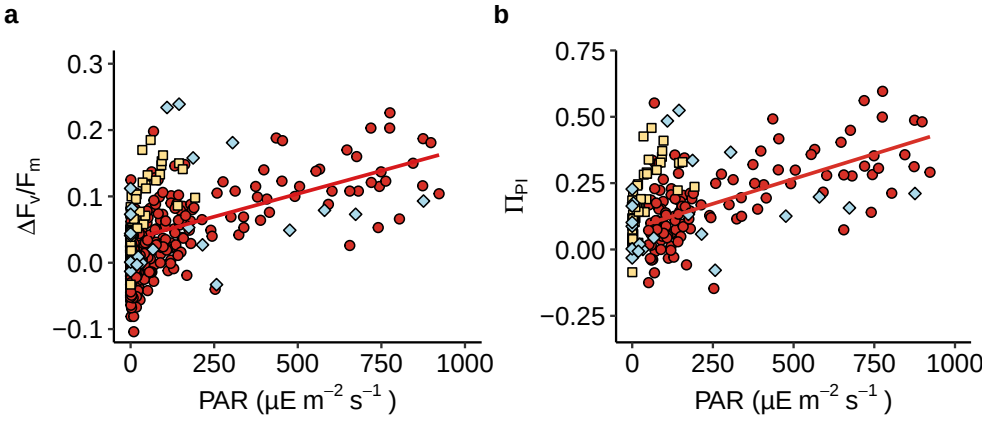

Figure 8 (a) $\Delta F_v/F_m$ and (b) Π_{PI} versus *in situ* PAR from the VERMIX-cruise (red, bullets), the Irminger Sea (brown, squares) and Sargasso Sea (blue, diamonds). Linear regressions to the the VERMIX-observations (>50 μE m^{-2} s^{-1}) are shown as red lines.